

A TEMPORARILY-CAPTURED ORBITER RENDEZVOUS EXPLORER & REMOTE SENSING MISSION

Arthur E. Chadwick^{a,1,*}, Adrienne N. Rudolph^{b,2,*}, Ananyo Bhattacharya^{c,2}, Ana Sofia Alonso^{a,3}, Nitya Jagadam^{d,6}, Claudio Toquinho Campana^{e,2}, Gianfranco Di Domenico^{e,2}, Inhae Lee^{a,3}, Siamand Lalisani^{a,1}, Azadeh Fathi^{a,1}, Max Luo^{a,3}, Mathieu Boyer^{a,4}, Zane Emery^{a,3}, Kaylin Borders^{a,1}, Matteo Calabrese^{a,1}, Steven Yang^{a,5}, Victor Lançon^{a,4}, Grace Genszler^{a,7}, Joshua Umansky-Castro^{a,7}, Andrew van Paridon^{a,8}, Elaine M. Petro^{a,8}, Dmitry Savransky^{a,9}, Mason A. Peck^{a,9}

^aCornell University, 130 Upson Hall, 124 Hoy Rd, Ithaca, New York, 14850, USA, (607) 255-3623

^bThe University of Maryland, 3181 Glenn L. Martin Hall, College Park, Maryland, 20742, USA, (301) 405-2376

^cUniversity of Michigan, Ann Arbor, MI, 48109, United States

^dUniversity of Illinois Urbana-Champaign, Urbana, IL, 61801, United States

^ePolitecnico de Milano, Via Giuseppe La Masa 34, Milano (MI), 20156, Italy

Abstract

The 2023 National Academy of Sciences, Engineering, and Medicine Decadal Survey on Planetary Science and Astrobiology lists several key questions regarding the collisional, dynamical, and physical evolution of small body populations in the solar system. Among those objects are Temporarily Captured Orbiters (TCOs), a subset of near-Earth objects (NEOs) that enter the Earth-Moon system and briefly orbit before leaving. TCOs remain largely unstudied, in part due to a lack of data from both ground- and space-based telescopes. TCOs present a unique opportunity for studying bodies external to the Earth-Moon system without the need for expensive deep-space missions to investigate them. This paper will present the mission concept of Mini-Luna, a cislunar mission designed by students from Cornell University's Smallsat Mission Design School (SMDS), tailored for NASA's Small Innovative Mission for Planetary Exploration (SIMPLEx) program. The Mini-Luna mission concept, with its 12U TCO Rendezvous Explorer (TReX) CubeSat, aims to demonstrate the viability of smallsat form factors for traveling to, rendezvousing with, and in-situ characterization of TCOs, thereby also addressing gaps in knowledge regarding the TCO population. Historically, no spacecraft has visited a TCO, highlighting the Mini-Luna mission as a novel scientific and technological pursuit. The TReX technology demonstration can also be a potential minimum viable product (MVP) for future small body targets.

Keywords: SmallSat, Mission Design, Near-Earth Objects, Temporarily-Captured Orbiters, Rendezvous

1. Introduction

Temporarily-Captured Orbiters (TCOs) are Near Earth Objects (NEOs) that stay within the Earth-Moon system for at least one geocentric orbit. These bodies are useful for study, and the Mini-Luna mission will consist of sending a small satellite to a TCO. TCOs provide a unique opportunity for low-cost

*Corresponding authors

Email addresses: ac2334@cornell.edu (Arthur E. Chadwick), rudo1pa@umd.edu (Adrienne N. Rudolph)

¹PhD Student, Mechanical & Aerospace Engineering

²PhD Student, Aerospace Engineering

³Masters Student, Mechanical & Aerospace Engineering

⁴Undergraduate Student, Mechanical & Aerospace Engineering

⁵Post-Doctoral Associate, Mechanical & Aerospace Engineering

⁶Masters Student, Aerospace Engineering

⁷PhD Candidate, Mechanical & Aerospace Engineering

⁸Assistant Professor, Mechanical and Aerospace Engineering

⁹Professor, Mechanical and Aerospace Engineering

space missions, as they require orders of magnitude of less delta-v than the traditional interplanetary travel to solar system bodies. Small-satellite technology is capable of meeting these TCOs to study their chemical, physical, and thermal compositions, paving the way for future smallSat missions to rendezvous with, study, capture, and potentially manipulate the orbits of TCOs. The act of a smallSat rendezvousing with a TCO is a novel technology capability, and studying the composition of TCOs can allow us to better understand the origins of the solar system. The following work covers the design of the Mini-Luna mission.

2. Science Background

2.1. Relevance to the NASEM Decadal Survey and Planetary Defense

The National Academy of Sciences, Engineering, and Medicine provides a decadal survey of high-priority science goals for Planetary Science and Astronomy. In the latest decadal survey titled “Origins, Worlds, and Life: A Decadal Strategy for Planetary Science and Astrobiology 2023-2032”, a comprehensive report of major scientific questions and important scientific exploration mission concepts guides the future of small-body exploration and associated technology development [1].

Small bodies such as asteroids, comets, and meteoroids are remnants of the origin and evolution of the solar system. The motion and interactions between these minor bodies composed of rock and ice drive the formation of planetary bodies, asteroid belt, and Kuiper belt objects. An understanding of their chemical composition and isotopic ratios are known to be key tracers for solar system evolution. Some prominent examples include the abundance of hydrogen and noble gas isotopes that serve as a cornerstone of geochemistry and the evolution of water in the solar system.

The current state of scientific understanding lacks data about minor bodies ranging in size from 1 to 10 meters. These bodies are expected to be fragments of collisions between relatively larger asteroid bodies, and serve as remnants for investigation of parent asteroid bodies and small body interactions within the solar system. The shape and surface properties provide additional information about small-body interactions and space weathering. From independent modeling efforts of Monte Carlo simulations, it is inferred that bodies in the same size range are expected to be captured as TCOs in Earth’s Hill Sphere. This presents a unique opportunity for the Mini-Luna mission to provide a wide range of scientifically relevant information about these objects. The decadal survey has proposed some important questions associated with the exploration of small bodies. Some of the key questions associated with small bodies similar to TCOs are listed as follows:

- Q4.1b How Has Collisional and Dynamical Evolution Affected Small Body Populations?
- Q4.1c What Are the Life Cycles (Physical States and Rotational Properties) of Small Bodies in the Solar System and How Are They Affected by Collisions, Thermal Changes, and Non Gravitational Forces?

Near-Earth Objects (NEOs) ranging in size distribution around 50-100 m are capable of causing regional destruction. These objects are capable of detonation in the atmosphere, depositing large amounts of energy, and potentially leading to Tunguska-scale events [2]. It is estimated that about 0.03 to 0.7 percent of these objects have been discovered [3]. TCOs, despite being small, are temporarily captured near Earth. Their proximity makes them much more accessible than most small bodies in the solar system, which are typically far away and require expensive missions to reach. This opportunity also aligns with the strategic goals of NASA Planetary Defense program enhancing the capabilities of NEO characterization and reconnaissance.

- 1.1 Continue to identify opportunities in existing and planned space domain awareness programs to improve detection and tracking by enhancing the volume and quality of current data streams, including from ground-based and space-based optical, infrared, and radar facilities.
- 1.7 Advance concepts for rapid characterization of a potentially hazardous NEO
- 3.1 Collaborate with interagency partners on technologies for rapid response, reconnaissance, and characterization of in-space objects. Evaluate the capabilities of current and projected launch vehicle infrastructure to support short-warning planetary defense missions.

2.2. Ground-based Detection of TCO's: Present Capabilities and Imminent Improvements

To date, most TCO detections have occurred through incidental observations rather than dedicated search efforts. This is largely due to the small size, low brightness, and short-lived nature of these objects. Although only two TCOs have been positively confirmed as natural satellites, many observatories involved in Space Domain Awareness (SDA) and the tracking of geocentric debris routinely collect tracklets and observational data that may include TCO candidates. These observatories often have secondary objectives aligned with Near-Earth Object (NEO) detection for planetary defense purposes. One of the most productive ground-based systems in this regard was the Space Surveillance Telescope (SST), which, over 103 nights between 2013 and 2017, detected 92 candidate objects as small as 25 cm—some of the smallest ever recorded in Earth orbit [4].

In addition, ground-based TCO detection capabilities are set to imminently improve with the Vera C. Rubin Observatory's Legacy Survey of Space and Time (LSST): "Small body populations throughout the Solar System will see an increase of 10-100 times more objects than currently known, including Earth mini-moon, irregular satellite, and cometary populations" [5]. Compared to the SST's 100 Megapixel camera, the LSST's 3.2 Gigapixel camera is a massive improvement, and it will be surveying nightly for 10 years capturing many orders of magnitude more images. Armed with "the largest digital camera ever constructed," the LSST is set to begin surveying by Q3 of 2025, and serves as the impetus behind Mini Luna seeking to launch by 2030 [5].

2.3. Science Traceability Matrix

We formulate a science traceability matrix (STM) consisting of two major scientific objectives. These objectives are guided by high level questions posed by the NASEM decadal survey. Below is a summary of each objective and its significance regarding the overall scientific goals. See the Appendix for the complete STM.

1. **Determine the size, shape and rotation rate of a TCO:** The structure of TCO can be quantified by its shape, size and surface roughness. An understanding of these physical quantities shall provide information about the TCO formation, and its evolution. A survey of these properties are also essential for developing an engineering model for future in-situ sampling and redirection tests.
2. **Characterize the surface composition of minerals and volatile compounds:** Information about surface composition will provide information about its nature. Generally asteroids are classified according to the inventory of organics, ice, and rocky minerals. A qualitative characterization of surface minerals and volatile abundance is important to understand the space weathering, and overall volatile inventory.

3. Mission Overview

We present the Temporarily Captured Orbiter Rendezvous Explorer (TReX), a 12U SIMPLEx class mission concept to rendezvous with and characterize a target TCO from its orbit at the Earth-Moon L_2 point. TReX has a multispectral imaging instrument to collect detailed data about the three-dimensional structure of the target, a mini-moon of size between 1 to 100 m.

We propose a mission development timeline according to the SIMPLEx solicitation for interplanetary missions. Per the SIMPLEx solicitation, the spacecraft must be launched within four years from solicitation approval [6]. TReX can leverage a rideshare program to the Earth-Moon L_2 point for start of operations. The entire mission development is divided into several phases with specific goals and objectives to be achieved in order to qualify for the next one. The order is as follows: Mission Concept Review (MCR), Mission Definition Review (MDR), Preliminary Design Review (PDR), Critical Design Review (CDR), and System Integration Review (SIR). The longest phase is expected to be Phase D, or the Assembly, Integration, and Testing phase, which also accounts for additional schedule slip and contingency.

The mission is organized into distinct development phases, with milestones that align with established aerospace industry standards and deliverables. If the rideshare program is to be facilitated by NASA's Gateway Artemis IV program, then it is important to acknowledge possible program and launch delays [7]. In such case, SpaceX's Starship also has the potential to provide a rideshare opportunity. Figure 1 shows the timeline for the design review process.

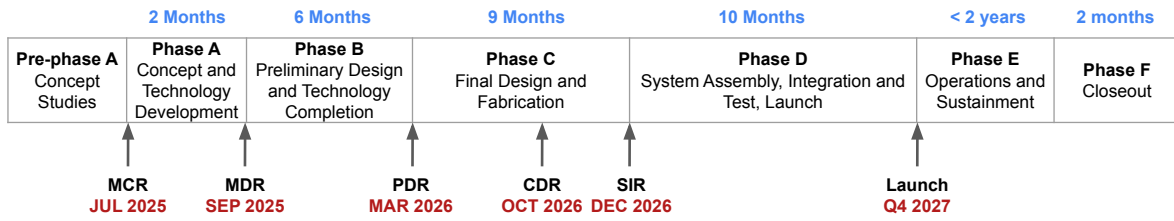


Figure 1: Mini-Luna Program Timeline.

Requirements drive the design of the mission, the spacecraft, and its subsystems. Table 1 highlights the high-level requirements of the Mini-Luna mission and its TReX spacecraft. Some of the requirements come from the SIMPLEx solicitation, which places a maximum cost or volume of the spacecraft. Additional requirements are derived from the mission’s guiding science questions, such as the measurable characteristics of the mini-moon and the time needed to complete measurements. Each subsystem has its own set of requirements driven by overall mission requirements.

Table 1: Mission Level Requirements.

ID	Requirement	Text
MIS 1	Lifetime	The mission shall have a lifetime between 2 and 5 years.
MIS 2	Cost	The mission shall cost no more than \$55 million.
MIS 3	Volume	Mini-Luna shall take up a volume no more than 12U.
MIS 3.1	Mass	Mini-Luna shall weigh less than 24 kg.
MIS 4	Target	Mini-Luna shall target a detectable mini-moon.
MIS 4.1	Target Estimation	Ground observation shall estimate the diameter of the TCO.
MIS 4.2	Minimum Target	TReX shall target a TCO at least 1 meter in diameter.
MIS 4.3	Maximum Target	The target mini-moon diameter shall be no greater than 100 m.
MIS 5	Composition	Mini-Luna shall determine the composition of the target in situ.
MIS 5.1	Proximity Distance	TReX shall match the target’s trajectory distance by no greater than 50 meters.
MIS 5.2	Proximity Duration	TReX shall conduct the science phase for at least 10 hrs.
MIS 5.3	Payload Pointing	TReX’s science payload shall be pointed at the TCO’s illuminated face.
MIS 5.3.1	Attitude Control	TReX shall control its position and attitude while imaging the TCO.
MIS 6	Mission Phases	The spacecraft shall have the following mission phases: 1. Launch and deployment, 2. Parking Orbit, 3. Rendezvous with asteroid and science, 4. Transmit Science Data and 5. End of Life and Decommissioning.
MIS 7	Rideshare	Mini-Luna shall travel to a parking orbit via a rideshare program.
MIS 8	Payload Data	TReX shall communicate payload data to the ground segment subsequent to science data capture and processing.
MIS 9	End of Life	TReX shall enter an appropriate EoL trajectory subsequent to confirmation of payload data receipt from the ground segment.

3.1. CONOPS and Story Board

The operation of TReX spacecraft beyond the launch to L_2 point will consist of several phases to achieve mission objectives. Figure 2 shows the mission concept of operations (CONOPS) in a story-board. The mission phases are as follows:

1. Launch and Deployment

- In this phase the spacecraft launches from a Starship or an Artemis IV rideshare vehicle to Earth-Moon L_2 and deploys its solar arrays upon separation.

2. Parking orbit station-keeping

- In this phase the spacecraft will transmit telemetry data for health monitoring and maintain its orbit using its chemical propulsion system.
- The spacecraft will also receive the TCO ephemerides (preloaded with NASA JPL’s Horizons database) and the required trajectory commands to meet the TCO and match its velocity.

3. Burn and Science Phase

- Once the TCO is selected, TReX will use its thrusters to rendezvous with the TCO and match its velocity.

- The thruster will then shut off, allowing the spacecraft to cool and use power to operate hyperspectral imager science instrument.

4. Data transmit and EOL

- TREx will then continue to follow the TCO and when it is closest to the Earth it will downlink the image data using the deployable dish antenna.
- TREx will then remain with the TCO until it leaves the Earth-Moon system.
- Once at periapsis around the Sun, TREx will be commanded over the Deep Space Network (DSN) to use the remaining propellant to slow down and minimize collision risk per NASA's Orbital Debris Mitigations Standard Practices [8].

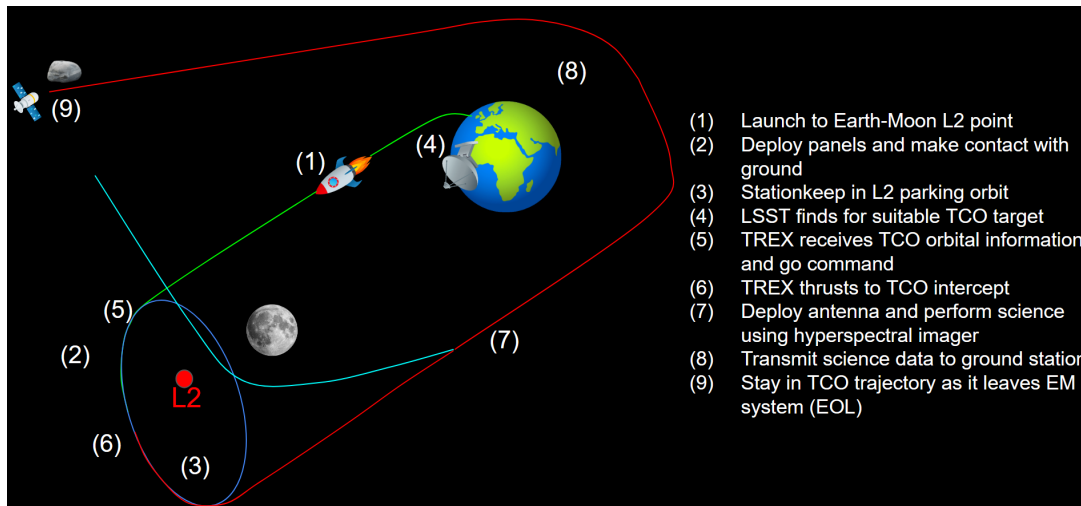


Figure 2: Mission Storyboard.

3.2. Trajectory

TREx's trajectory can be subdivided in two main phases.

- The first stage of the mission's trajectory begins when TREx is deployed from the rideshare launch vehicle and maneuvers to an orbit around the Earth-Moon L_2 (EML_2) Lagrangian point. The spacecraft will be placed in a quasi-stable periodic orbit, such as a halo orbit or a Lyapunov orbit, around EML_2 . Compared to low lunar orbits, these orbits require significantly fewer station-keeping maneuvers. A properly chosen orbit around EML_2 provides near-continuous communication with Earth, as the spacecraft remains within Earth's line of sight. The expected orbital period is approximately 9 days, depending on the specific orbit selected.
- The second stage consists of executing the required maneuvers to rendezvous with an asteroid. These maneuvers include, but are not limited to, departing from the Earth-Moon L_2 point, adjusting the orbital inclination, performing an elliptical transfer from the post- L_2 departure position to the rendezvous trajectory, and placing the TCO on a hyperbolic escape path while accelerating to match the target TCO's velocity. This phase is expected to take up to one year.

There are a variety of types of potential parking orbits for EML_2 . Orbit types can be divided into orbit families, northern or southern, Jacobi constant, period, and stability index. Over time, spacecraft deviate from an intended trajectory if initial calculations are based on the circular-restricted three body problem (CR3BP) model, which does not take into account forces such as the rest of the planets, solar radiation pressure, etc. Halo and Lyapunov orbits are the two main parking orbits considered. The stability index is a key feature of an orbit because it quantifies the energy needed to stay within the orbit itself. A low stability number means less delta-v required to station-keep in that orbit, with a downside being that the orbit itself is closer to Earth and thus more delta-v would be required to orbit raise and change inclination to the TCO. TREx could be in an EML_2 Halo orbit with a low stability index; these orbits are usually perpendicular to the Earth-Moon plane, are highly elliptical, and have a periapsis that is very close to the Moon. On the other hand, a higher stability index (less stable) orbit such as an EML_2

Lyapunov orbit would reach closer to the TCO's trajectory, thus requiring less delta-v to orbit raise. Additionally, orbiting in the Earth-Moon plane requires no initial inclination change to complete the orbit raise CONOPs, unlike the Halo orbit.

Mini-Luna relies on the target TCO ephemerides from Earth based observations, and sky surveys. The Catalina Sky Survey and Asteroid Terrestrial-impact Last Alert System have the capabilities to detect and monitor TCO in Earth-Moon system. In near future, the Large Synoptic Survey Telescope (LSST) will also aid in discovery and tracking of a major proportion of TCOs. The ephemerides will be updated based on latest observations, and the trajectory will need to be adjusted for each specific TCO to support the mission during rendezvous phase. A sample trajectory for a rendezvous with the 2006 RH120 TCO in October 2028 is provided in this paper. This mission approach is similar to what was previously adopted for the Comet Interceptor mission [9], which is to send a spacecraft to the Earth-Sun L_2 and wait for a suitable target comet to be identified in order to intercept it.

3.3. Case Studies

The process of choosing a TCO is intricate. First, the asteroid must meet the following criteria to be classified as a TCO [10]:

1. The Keplerian energy with respect to Earth must satisfy $E_{\text{Earth}} < 0$.
2. The distance from Earth to the body must be less than three Earth Hill radii, ~ 0.03 AU.
3. The body must complete at least one full revolution around the Earth.
4. The TCO's diameter must be between 1 and 100 m.

Based on these criteria, several TCO candidates listed were identified.

Table 2: Potential TCOs.

Name	Diameter [m]	Approach Relative to L_2		
		Distance [km]	Velocity [km/s]	Date
2006 RH120	$\sim 2\text{-}10$	$4.17 \cdot 10^6$	0.29	10/27/2028
2020 CD3	$\sim 1\text{-}4$	$1.36 \cdot 10^6$	0.96	2/3/2020
2022 OB5	$\sim 3\text{-}13$	$1.97 \cdot 10^6$	1.70	1/24/2026
2024 PT5	~ 10 [11]	$1.07 \cdot 10^6$	1.76	7/31/2024
2024 YR4	$\sim 40\text{-}90$ [12]	$7.82 \cdot 10^6$	12.98	12/17/2028

Many open databases provide information on small-body observations and their derived ephemerides. The JPL Small-Body Database, IAU Minor Planet Center Orbit Database, and AstDyS database archive valuable data on near-Earth objects (NEOs) and close-approach opportunities. Additionally, NASA JPL's Horizons database offers ephemerides, including the relative position and velocity of NEOs [13]. This database was utilized in the trajectory analysis presented in Table 2.

When computing the delta-V required for a rendezvous with a TCO, the relative distance and velocity of the TCO with respect to L_2 play a crucial role in determining feasibility. After evaluating the different target TCOs, 2006 RH₁₂₀ was chosen due to its past and future close approaches, its low relative velocity, its low relative inclination change, and its breadth of previous literature.

The rendezvous mission concept trajectory consists of three burns, plotted in the inertial or geocentric frame in Figure 3, as well as the Earth-Moon rotating frame in Figure 4. The axes are measured using lunar distance (LD). The first burn places the spacecraft on a trajectory to escape the EML₂ point and enter the Earth's sphere of influence. The second burn executes the first half of a Hohmann transfer, expanding the spacecraft's Earth-centered orbit along an elliptical trajectory to intersect the TCO's path. This second burn will also involve an inclination change to match the TCO's orbit plane. The third burn adjusts the spacecraft's orbit, first circularizing it and then expanding it further to match the TCO's hyperbolic trajectory. All three burns in Equation (1) are added together to establish the total delta-v needed for the mission.

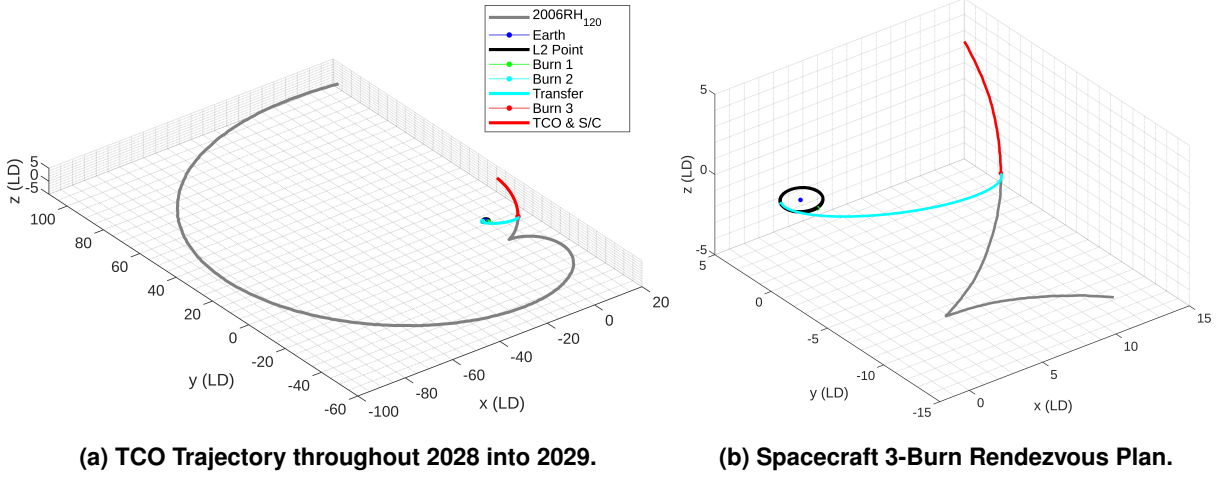


Figure 3: Trajectory to TCO in Inertial Frame.

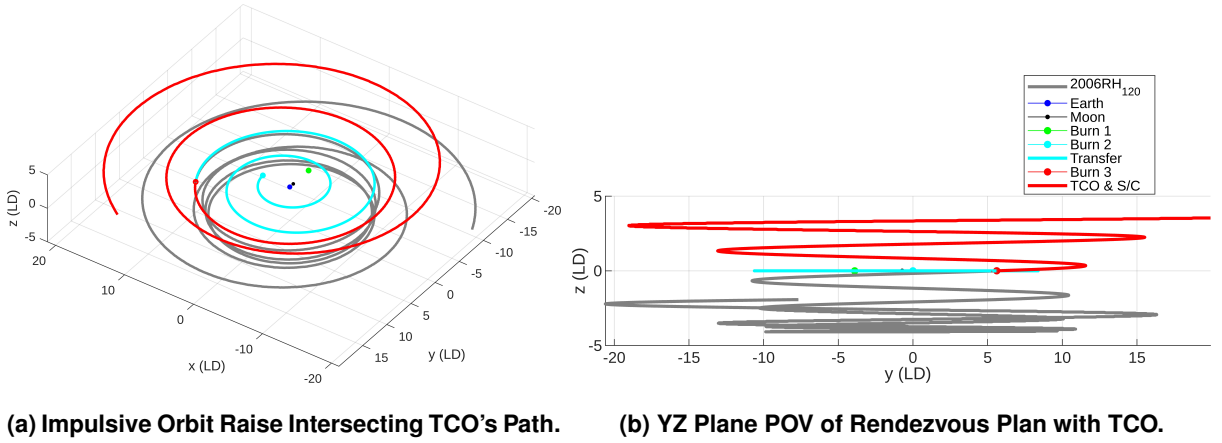


Figure 4: Trajectory in Earth-Moon Rotating Frame.

$$\Delta v_{total} = \Delta v_{Burn 1} + \Delta v_{Burn 2} + \Delta v_{Burn 3} \quad (1)$$

The rendezvous trajectory with TCO 2006 RH120, with a rendezvous date of October 28th, 2028, begins with the spacecraft in a Near Rectilinear Halo Orbit (NRHO) about the L_2 point. The initial velocity of EML_2 relative to the Earth, v_{L_2} , is calculated using Equation (2), where v_{esc} is the velocity needed to escape the L_2 point.

Equation (3) expands each term, where μ_{EM} is the Earth-Moon gravitational constant and r_{L_2} is the radius that L_2 orbits around the Earth. It is assumed the spacecraft is at the L_2 point for the start of the trajectory. The goal is to get the spacecraft away from the Moon and L_2 enough to where the dominant sphere of influence is only the Earth. The radius of L_2 about Earth is approximately $1.5 \cdot 10^9$ km, while the intersection of 2006 RH₁₂₀'s trajectory is about $4.17 \cdot 10^9$ km. Burn 1 equals 114 m/s.

$$\Delta v_{Burn 1} = v_{escape L_2} - v_{L_2} \quad (2)$$

$$\Delta v_{Burn 1} = \sqrt{\frac{\mu_{EM}}{r_{L_2}}} (\sqrt{2} - 1) \quad (3)$$

For Burn 2, the spacecraft needs to orbit raise away from Earth such that the orbit intersects the TCO's trajectory. This calculation can be done using the first part of a Hohmann transfer, which expands the orbit from circular to elliptical. The radial position of the L_2 point relative to Earth is assumed to be constant and is noted as r_{L_2} in Equation (4). The velocity needed to complete the transfer orbit in Equation (5) is a function of the semi-major of the transfer. The TCO's trajectory can be assumed to be

a radius around Earth as well, noted as r_{TCO} . The already known initial velocity of the spacecraft is the L_2 point velocity. Burn 2 equals 110 m/s.

$$\Delta v_{Burn\ 2} = v_{transfer} - v_{L_2} \quad (4)$$

$$\Delta v_{Burn\ 2} = \sqrt{\frac{2\mu_{EM}}{r_{L_2}} - \frac{\mu_{EM}}{\frac{(r_{L_2}+r_{TCO})}{2}}} - \sqrt{\frac{\mu_{EM}}{r_{L_2}}} \quad (5)$$

The elliptical transfer required to raise the orbit and match that of the TCO's trajectory will take approximately 275 days. This transfer is half of the orbit period of the elliptical orbit, as shown in Equation 6.

$$T_{transfer} = \frac{T_{elliptical\ orbit}}{2} = \frac{\sqrt{\frac{4\pi^2 a^3}{GM}}}{2} \quad (6)$$

Burn 3 is the most complex burn in the rendezvous. It is divided into three parts, as shown in Equation (7). The first part accounts for the inclination change, since it is highly unlikely that the TCO will orbit in the same plane as the Moon. The second part circularizes the orbit around Earth. The third part continues to expand the orbit until it becomes hyperbolic and thus matching the TCO's energy.

$$\Delta v_{Burn\ 3} = \Delta v_{inclination\ change} + \Delta v_{circularize} + \Delta v_{hyperbolic} \quad (7)$$

The $\Delta v_{inclination\ change}$ accounts for angle difference between the TCO's orbit and the plane that the spacecraft is currently in. The angle in degrees n , the maneuver raising increment Δi , and initial velocity are used in Equation (8). The angle change needed is approximately 20 degrees and the maneuver changing increment was set to 20 as well. The inclination change burn results in 78 m/s of delta-v.

$$\Delta v_{inclination\ change} = n v_{transfer} \sin \frac{\Delta i}{n} \quad (8)$$

The circularizing velocity shown in Equation (9) is the second half of the Hohmann transfer formula, where the spacecraft expands the ellipse back into a circular orbit but larger. The circularizing delta-v equals 84 m/s.

$$\Delta v_{circularize} = \sqrt{\frac{\mu_{EM}}{r_{TCO}}} - \sqrt{\frac{2\mu_{EM}}{r_{TCO}} - \frac{\mu_{EM}}{\frac{(r_{L_2}+r_{TCO})}{2}}} \quad (9)$$

From the now circularized orbit, the spacecraft must expand the radius further to get close to a hyperbolic orbit, as that is the behavior of the TCO. This continued velocity added is the same formula structure used to leave L_2 in Burn 1 and is shown in Equation (10). The hyperbolic delta-v maneuver equals 128 m/s.

$$\Delta v_{hyperbolic} = \sqrt{\frac{\mu_{EM}}{r_{TCO}}} (\sqrt{2} - 1) \quad (10)$$

Equation (11) collects each critical function needed to complete the last leg of the rendezvous. Burn 3, which includes the inclination change, circularizing, and hyperbolic maneuver, equals 290 m/s.

$$\Delta v_{Burn\ 3} = n \sin \frac{\Delta i}{n} \sqrt{\frac{2\mu_{EM}}{r_{L_2}} - \frac{\mu_{EM}}{\frac{(r_{L_2}+r_{TCO})}{2}}} + \sqrt{\frac{\mu_{EM}}{r_{TCO}}} - \sqrt{\frac{2\mu_{EM}}{r_{TCO}} - \frac{\mu_{EM}}{\frac{(r_{L_2}+r_{TCO})}{2}}} + \sqrt{\frac{\mu_{EM}}{r_{TCO}}} (\sqrt{2} - 1) \quad (11)$$

All three burns (Burn 1, Burn 2, and Burn 3) together equal a total delta-v of 514 m/s. Considering the delta-v required for station-keeping maneuvers in the EM L_2 , estimated at 7.39 m/s per year [14], a total of 15 m/s may be needed for a two-year mission. Consequently, the total delta-v required for the mission amounts to 529 m/s.

4. Spacecraft Design

4.1. Scientific Instrument

The current scientific questions warranted a trade investigation on the type of scientific instrument fit for the posed objectives. Characterization of TCO surface features, and elemental composition can be performed by analyzing the spectra of sunlight reflected from the TCO surface. This can be achieved using a multispectral imaging instrument. Given the characteristic rotation period of target TCOs, the instrument will be able to survey its surface over several rotation periods from an optimal viewing angle.

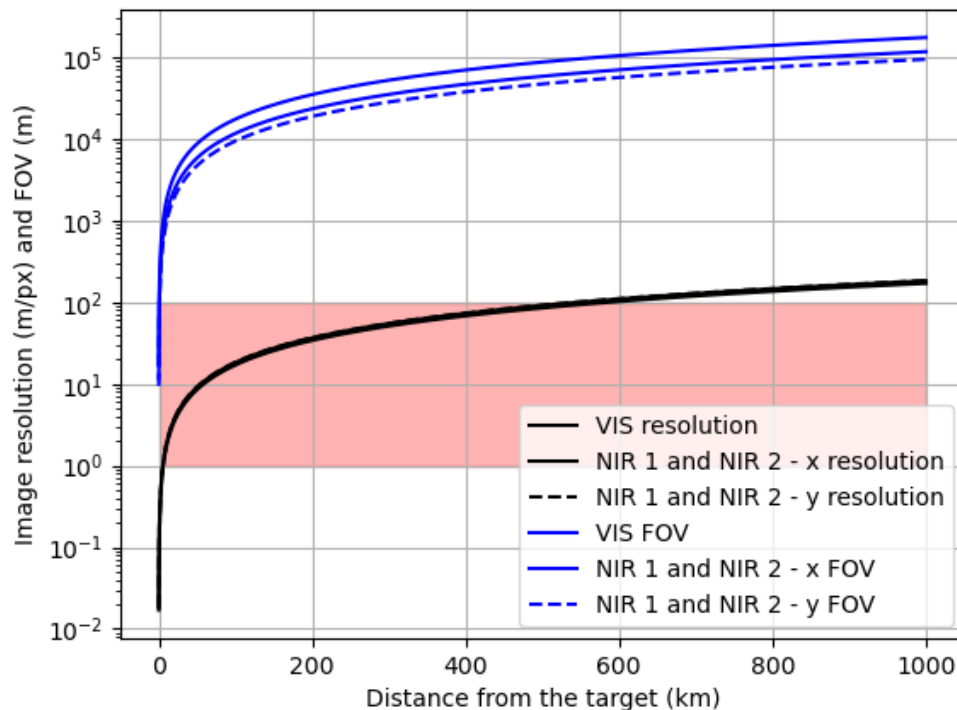


Figure 5: The field of view (FOV) (m) and image resolution (m) for multispectral imaging instrument as a function of TReX distance to target TCO. The red rectangle highlights the nominal target size relative to image resolution. At distance between 100 and 1000 km, the imager can also be used for navigation purposes.

Table 3: ASPECT Specifications [15].

Channel	VIS	NIR1	NIR2	SWIR	Units
Field of View	10 x 10	6.7 x 5.4	6.7 x 5.4	5 circular	deg
Spectral Range	500 - 900	850 - 1275	1225 - 1650	1600 - 2500	nm
Image Size	1024 x 1024	640 x 512	640 x 512	1 x 1	pixels
Pixel Size	5.5 x 5.5	15 x 15	15 x 15	1000 x 1000	μm
Spectral Resolution	<20	<40	<40	<40	nm

For the multispectral imager, we propose the Multispectral Imaging Instrument (MII) based on the ASPECT instrument onboard Hera Juventus cubesat. It consists of four bands: VIS, NIR1, NIR2 and SWIR covering a wavelength range between 500-2500 nm. It uses tunable Fabry Perot Interferometers to select the image wavelengths and form a spectral datacube. The VIS and NIR channels are imaging spectrometers while the SWIR channel is a single pixel spectrometer. The technical specifications of the MII in Table 3 are based on ASPECT multispectral imaging cameras onboard the Hera Milani cubesat [15]. We aim to measure the reflectance spectra from the rotating surface at a range of optimum solar zenith angles. These bands provide a high-resolution spectra of surface minerals and space weathering, that can be complemented by machine learning techniques for surface characterization [16, 17]. The synthesis of data cubes will help us in TCO taxonomy supported by spectroscopy of various asteroid mineral analogues [18].

Figure 6 below displays the apparent size of a TCO such as 2006 RH120 from the perspective of an observer, or in this case, the TReX spacecraft. The potential size of 2006 RH120 from Table 2 ranges from 2 to 10 meters in diameter, which were used as the lower and upper bound for the angular size analysis below.

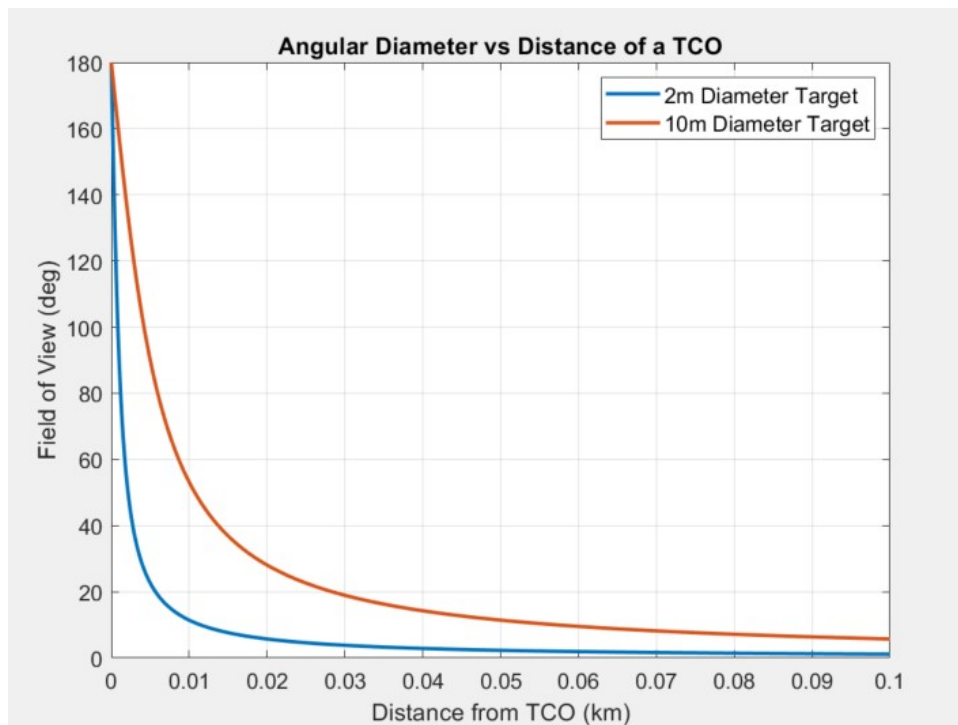


Figure 6: The apparent angular size (in degrees) of TCO 2006 RH120 as a function of spacecraft distance away from the body

This analysis reveals the minimum field of view required for an instrument to capture the entire TCO at a given distance. If the TCO (such as 2006 RH120) is on the smaller end (2-meter diameter), TReX must be closer to the asteroid compared to if the asteroid were larger (10-meter diameter). These insights help us determine how close we need to position our cameras to ensure the asteroid remains fully within view.

4.2. Data Processing

Multispectral imaging generates substantial volumes of data, with each image producing approximately 50 megabits. Additionally, the specific operational profile of TReX depends on the trajectory and physical characteristics of the target TCO. These target parameters define the onboard data storage and processing requirements, as different TCOs may require varying numbers of measurements, affecting the total data volume.

Due to uncertainties in the spacecraft's line of sight, atmospheric conditions, and distance to ground stations during downlink opportunities, it is essential to ensure that all scientific data can be stored onboard until conditions allow for efficient transmission. This approach helps prevent potential scientific data loss. Scientific data handling, transmission, and storage differ significantly from the transmission of telemetry, tracking, and command (TT&C) data. While scientific data volumes are expected to reach the order of gigabits, telemetry and spacecraft state-of-health (SOH) data are typically in the kilobit range. The frequency of transmission also differs: telemetry data is expected to be downlinked at least once per day, whereas scientific data will be stored and transmitted opportunistically when conditions permit.

Given these differing requirements, the system was designed to support parallel data streams and accommodate high-capacity storage. Additional selection criteria included the use of components with a Technology Readiness Level (TRL) of 6 or higher, low power consumption, and support for a variety of instrument interfaces. These considerations led to the selection of the onboard processor, primarily driven by two key features: its embedded storage capacity of up to 256 gigabytes, and its low-power,

dual-core ARM-based architecture. Table 4 summarizes the processor’s technical specifications. To provide redundancy and improve fault tolerance, three processors will be included. A cold redundancy scheme will be implemented, in which two processors remain on and the backup processor remain off and is activated only in the event of a failure or, in rare cases, when maximum storage capacity is reached.

Table 4: Data Processing Specifications.

Specification	Value
Processor Amount	Triple Redundancy
Power Consumption	5 W
Processor Type	500 MHz dual-core
RAM Memory	4GB DRAM
Flash Memory	2x 256 MB NOR

4.3. Attitude Determination & Control System

The Attitude Determination and Control System (ADCS) is in charge of ensuring 3-axis pointing capabilities to the spacecraft throughout the mission. The system shall first precisely determine the attitude of the spacecraft and then act accordingly to achieve the desired orientation and maintain it stable during the science. The proposed ADCS devices ensure fulfilling instruments’ requirements. The control devices shall be sized about the most stringent modes, thus guaranteeing operational capabilities in all possible mission conditions. Redundancy shall be also ensured to mitigate possible unforeseen circumstances and provide fault tolerance margins. A high level of autonomy shall be ensured to lower operational costs and enhance promptness in critical phases.

Mission objectives and concept of operations naturally define the requirements the ADCS subsystem shall satisfy. Since the spacecraft will be orbiting for most of the time about the Lagrange 2 point of the Earth–Moon system, control actuation and state determination cannot exploit the magnetic field of the Earth. Main control is therefore entrusted to three reaction wheels disposed in pyramidal configuration. The sizing of the reaction wheels is performed to eliminate a maximum rotational angular velocity of 10°/s per axis. Wheel de-saturation is achieved by actuation of a microthruster system, that can be also used as additional source of thrust during firing of the main engines. Furthermore, the RCS microthrusters are foreseen to perform initial de-tumbling at release from the carrier.

Attitude determination is essential to ensure the precise orientation of the spacecraft during operative scenarios. In particular, the spacecraft needs to direct its antennas’ boresights toward the Earth for TT&C purposes, align its solar panels along the Sun direction for power generation, and precisely point instrumentation during the science phase. Inertial attitude determination is principally achieved by the use of star trackers, two for redundancy. Because of the beneficial continuous illumination conditions assured by orbiting about the Lagrange 2 point, a Sun sensor contributes to the overall estimation of the spacecraft’s attitude. An Inertial Measurement Unit (IMU) completes the package of sensors. An Extended Kalman Filter is entrusted to signal processing thus output an accurate real-time estimation of the spacecraft attitude. However, the adoption of a Unscented Kalman Filter will be assessed at later phases of the design process. This filtering algorithm would enhance navigation and pointing accuracy during rendezvous with the TCO and science phase, where nonlinearities intensify, at the expense of higher computational power and time.

Table 5: ADCS Subsystem Specifications.

Component	Quantity	Comments
Reaction Wheels	4	Max momentum 0.1 Nms, max torque 0.007 Nm
Microthrusters	1	5 within system, nominal thrust 10 mN, R134a
Star Tracker	2	Cross/about 6/40 arcsec (1σ), 5 Hz sampling, max slew rate 2°/s
Sun Sensor	2	Accuracy $<0.5^\circ$ (3σ), precision $<0.1^\circ$, FOV $\pm 75^\circ$
IMU	2	Time to valid data 0.7s, input range $\pm 400^\circ/s$

Table 5 summarizes the actuators and the sensors that have been selected for the mission. All components are off-the-shelf and space flight proven to enhance reliability. Later analyses establish

whether the scientific payload may be exploited for attitude and navigation determination purposes as well.

4.3.1. Feedback Control Loop

The ADCS subsystem must control the distance between the TCO and the spacecraft during the science phase. Figure 7 shows the feedback control loop necessary to complete this "station-keeping" for the duration of the data collection. The information from the scientific instrument's imaging resolution and the ADCS subsystem must work together to obtain the required imagery data. The commanded attitude control rates for each axis are represented as $\tau_{commanded}$.

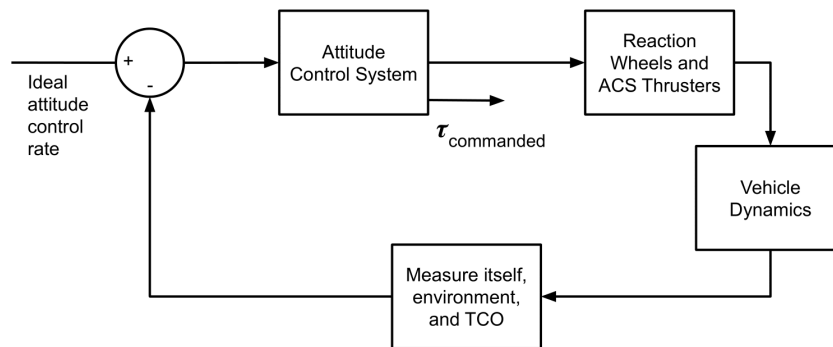


Figure 7: ADCS Feedback Control Loop.

4.4. Propulsion and Launch Vehicle

The launch vehicle should be capable of getting into a trans-lunar injection (TLI). Examples of possible launch vehicles are NASA's SLS and SpaceX's Starship. The launch vehicle would likely need to be partnered with through a rideshare program. NASA's Artemis program has mentioned plans for such a rideshare program.

The on-board propulsion requirements are driven by the need to rendezvous with the TCO target. The propulsion subsystem is responsible for following the nominal trajectories of escaping EML_2 , orbit raising, changing inclination, and hyperbolic maneuvers. Although used for electric propulsion applications, the well-known formula for estimating propellant mass as a function of other propulsion system variables is used in Equations (12) through (14). The mass of the system decreases after each burn and thus the propellant mass must be calculated starting with the last burn. Three burns are to be completed: Burn 1 to leave EML_2 , Burn 2 to orbit raise, and Burn 3 to change inclination, circularize its orbit, and expand its orbit to a hyperbolic trajectory to match the TCO. After accounting for each burn and using a specific impulse of 220 s, the total required propellant mass is 3.081 kg. The hydrazine thruster has a thrust F_{th} of 0.3 to 1.1 N, as well as a mass flow rate \dot{m} of 0.14 to 0.45 g/s.

$$m_{p3} = m_{dry\ mass} \left(e^{\Delta v_3 / (I_{sp} g)} - 1 \right) \quad (12)$$

$$m_{p2} = (m_{dry\ mass} + m_{p3}) \left(e^{\Delta v_2 / (I_{sp} g)} - 1 \right) \quad (13)$$

$$m_{p1} = (m_{dry\ mass} + m_{p2} + m_{p3}) \left(e^{\Delta v_1 / (I_{sp} g)} - 1 \right) \quad (14)$$

Table 6: Propulsion Overview.

Variable	Value					Units
Maneuver Type	Parking Orbit	Burn 1	Burn 2	Burn 3	All	-
Maneuver Date (t)	-	1/1/28	1/26/28	10/27/28	-	-
Wet Mass pre-Maneuver	13.751	13.009	12.331	10.708	-	kg
Delta-V with 5% Margin (Δv)	7.76	119.70	115.50	304.50	547.46	m/s
Propellant Mass (m_p)	0.038	0.742	0.678	1.623	3.081	kg
Total Firing Time (t_{Burn})	0.097	1.866	1.705	4.081	7.749	hrs

Literature provides a similar 12U lunar cubesat example to help in determining the parameters of TReX's propulsion system, where its mission requirements stated a maximum of 8 hours per burn [19].

TREx should adhere to this requirement and thus constrains the largest delta-v burn, burn 3 of 1.623 kg of propellant, to 8 hours, thus influencing the design choice's minimum mass flow rate. A Commercial Off-The-Shelf (COTS) monopropellant hydrazine (N_2H_4) thruster capable of this mass flow rate has a volume of approximately 1.35 U. More details on the propulsion system are found in Table 6.

4.5. Communications & Ground System

Communicating with a spacecraft at the Earth-Moon L_2 point poses significant challenges, especially for a CubeSat. The reliance on COTS components, which are primarily designed for Low Earth Orbit (LEO) operations, can severely impact communication quality. Additionally, strict Size, Weight, and Power (SWaP) constraints limit the available options for the communication subsystem. A further challenge arises from the mission's need to rendezvous with an asteroid, likely placing the spacecraft beyond the operational range of the Near Space Network (NSN). As a result, the spacecraft must be equipped to transition from NSN to the DSN after leaving the parking orbit.

Whilst in the L_2 parking orbit, the spacecraft will conduct Telemetry, Tracking, and Command (TT&C) operations via NSN. However, once the spacecraft travels beyond the Earth-Moon L_2 point, it will need to switch to DSN to maintain communications during the rendezvous maneuvers. At this stage, data transmission will be crucial not only for telemetry and command but also for high-speed scientific data transfer. In the case of the 2006 RH120 case study presented in this paper, rendezvous would occur at 4.17 million kilometers from Earth, exceeding the NSN's maximum range of 2 million kilometers. Consequently, Deep Space Network (DSN) becomes the only viable option for maintaining communications. TREx will be equipped with two distinct antennas: one for S-band communication with the NSN and another for X-band communication with the DSN.

The link budget for NSN was calculated using the specifications of White Sands Ground station. This station has an 18 m diameter antenna with a G/T value of 29.6 dB/K and an antenna gain of 50 dBi in S-band and a G/T of 46.98 dB/K. Since TT&C requires a low data rate (1-10 kbps), S-band was selected. This lower frequency band was chosen for its reduced pointing precision requirements and lower susceptibility to atmospheric attenuation.

For DSN communications, the specifications of the communication subsystems will be determined based on the four antennas that each ground station is required to have. The DSN consists of three ground stations strategically positioned 120 degrees apart in longitude to provide continuous coverage. These stations are located in Canberra, Australia; Madrid, Spain; and Barstow, California, USA. Each facility is equipped with two 34-meter diameter antennas, one 26-meter diameter antenna, and one 70-meter diameter antenna.

Table 7: Communications Subsystem Overview.

Data Type	Network	Band	Frequency	Data Rate	Contact Rate	Atmospheric Interference
TT&C	NSN ie: White Sands Gain: 50 dB G/T: 29.6 dB/K	S-band	2.2 GHz	<10 kbps	Near- Continuous for health data	Less susceptible
Scientific Data	NSN ie: Madrid, Canberra, California Gain: 74.8 dB G/T: 47 dB/K	X-band	8.4 GHz	<1 Mbps (<3 hours for 8 Gb)	Beyond NSN range during asteroid rendezvous	More susceptible

For science payload data transmission, TREx must be equipped with an antenna capable of transmitting data at 1 Mbps. The decision to use X-band for this purpose is driven by its balance between available bandwidth, low atmospheric attenuation, and well-established deep-space communication infrastructure, ensuring reliable and efficient data transmission over long distances. A summary of the communications subsystem is provided in Table 7, using data adapted from NASA's DSN specifications [20].

4.5.1. Link Budget Analysis

Table 8: Link Budget.

Data Type	Parameter	S-Band Value	X-Band Value	Units
Orbit Parameters	Elevation Angle	10	0	deg
	Distance	1,505,257	1,506,364	km
Transmitter Parameters	Frequency	2.2	8.4	GHz
	Wavelength	0.1362692991	0.03568957833	m
	Bit Rate	0.001	1.000	Mbps
	Transmit Power	3.2	2.0	W
	Transmit Power	34.99687083	33.01029996	dBm
	Transmit Antenna Gain	0	10	dBi
	Transmit System Losses	-4	-4	dB
	EIRP	30.99687083	39.01029996	dBm
	Path Loss	-222.85	-234.49	dB
	Receiver Parameters	Receive Antenna Diameter	18.2	70
Antenna Efficiency		60	65	%
Receive Antenna Gain		50.0	74.3	dBi
Noise Temperature		109.6	25.0	K
Receive System Noise Figure		-178.20	-184.62	dBm/Hz
Total Received Power		-137.9	-117.2	dBm
Receiver System Losses		-4	-2	dB
Cross Polarization Loss		0	0	dB
Link Margin Computation	Received E_b/N_0	10.4	7.4	dB
	Required E_b/N_0	3.0	3.0	dB
	Link Margin	3.4	2.4	dB
	Required Link Margin	2	2	dB

To validate the feasibility of the proposed communication architecture, two link budget analyses were performed for both the S-band and X-band links. The S-band budget accounts for TT&C operations via NSN. The X-band budget considers high-data-rate scientific transmissions via DSN, leveraging the 70-meter ground station antenna. The results of these calculations are summarized in Table 8. Constants that were used in the calculations included the radius of Earth = 6,378 km, altitude of satellite = 1,500,000 km, speed of light = 299,792,458 m/s, and Boltzmann constant = 1.38×10^{-23} W/K/Hz.

4.6. Power

The power subsystem for this CubeSat, designed to rendezvous with a temporarily captured object (TCO) from a lunar parking orbit, must be efficient and highly reliable. To meet these requirements, the spacecraft is equipped with three 6U solar panel arrays to convert solar power into electrical energy. These arrays are complemented with rechargeable lithium-ion batteries, which store excess energy and provide uninterrupted power during eclipses or mission phases of high-demand operation.

The electrical power system (EPS) is responsible for supplying energy to all critical subsystems, including propulsion, where approximately 18 W is required to actuate the thruster valves in the case of chemical propulsion, as well as the attitude determination and control system (ADCS), communications, and payload instrumentation.

Given the time-varying nature of spacecraft operations, the power demand is characterized by distinct mission phases: standby mode, propulsion burns, science operations, and data transfer. Table 9 summarizes the peak power usage and corresponding duty cycles for each subsystem across these operational modes. For instance, the science phase exhibits the highest total power consumption at approximately 52.90 W, driven largely by payload operation and attitude control components. In contrast, the standby mode operates at a baseline load of approximately 21.50 W. Data transmission phases, which rely on high-duty-cycle communication equipment, draw up to 38.90 W.

To accommodate these fluctuations, the EPS implements phase-based energy scheduling and load management strategies. During low-demand periods (e.g., standby or sunlight-rich data transfer win-

dows), the system prioritizes battery charging. Conversely, during peak-demand phases such as propulsion maneuvers or science observations, the batteries are discharged to supplement solar input. Battery cycling is managed to minimize deep discharge events, maintaining the state of charge within safe operational margins to maximize battery lifespan. The goal is to always maintain a state of charge of 30% or more. The batteries include 1 motherboard and 3 daughterboards to equal a 40 Wh capacity. The distributor module is capable of distributing up to 50 W. Three 6U solar panels provide the necessary power among all phases, assuming end of life (EOL) power capabilities of 17.70 W per panel.

Table 9: Power Budget per Mission Phase.

Subsystem	Component / Use Case	Peak Power (W)	Qty	Total Power (W)	Standby Mode		Burn Phase		Science Phase		Data Transfer	
					Duty Cycle	Power (W)	Duty Cycle	Power (W)	Duty Cycle	Power (W)	Duty Cycle	Power (W)
CD&H	Processor	5	3	15	67%	10	67%	10	67%	10	67%	10
Comms	S-Band Antenna	4	2	8	50%	4	50%	4	0%	0	50%	4
Comms	X-Band Antenna	4	2	8	0%	0	50%	4	50%	4	50%	4
Comms	Transceiver	12	2	24	10%	2.4	25%	6	50%	12	50%	12
ADCS	Reaction Wheels	1	4	4	10%	0.4	75%	3	75%	3	75%	3
ADCS	Microthrusters	10	1	10	10%	1	10%	1	40%	4	10%	1
ADCS	Star Tracker	1.5	2	3	50%	1.5	20%	0.6	50%	1.5	50%	1.5
ADCS	Sun Sensor	0.2	2	0.4	50%	0.2	20%	0.08	100%	0.4	100%	0.4
ADCS	IMU	1.5	2	3	0%	0	20%	0.6	100%	3	100%	3
Power	Deploy Solar Array	2	1	2	100%	2	100%	2	50%	1	0%	0
Propulsion	Actuate Thrust Valve	18	2	36	0%	0	50%	18	0%	0	0%	0
Payload	Hyperspec. Imager	14	1	14	0%	0	0%	0	100%	14	0%	0
Total Power (W)				127.40		21.50		49.28		52.90		38.90

4.7. Thermal and Environmental Protection

As cubesat complexity and power demands grow, effective thermal management design is increasingly essential. The communications transceiver, onboard computer, and propulsion systems are the primary contributors to internal thermal power generation to the TReX spacecraft due to the combination of usage time and estimated thermal dissipation. The subsystems with the narrowest operating ranges are the hyperspectral imaging subsystem and the battery. The imaging subsystem has the narrowest operating temperature range, from 0 to 20 °C, but it is only active during the science phase of the mission. In contrast, the battery, which operates between 0 °C and 40 °C, must remain within this range for the entire mission duration.

TReX subsystem temperatures will be managed through both passive and active systems. Because the spacecraft will receive constant sun exposure throughout the majority of the mission, the passive system will include potassium silicate painted panels covering the entire spacecraft body which has both low absorptivity of ~0.2 and high emissivity of ~0.9. In addition, passive thermal control will include thermally conductive straps connecting components with high thermal dissipation like the onboard computer and radio transceivers to the external panels.

Table 10: Thermal Power Dissipation (TPD) & Operating Temperatures.

Subsystem	Component (TPD W)	Min °C	Max °C	Mission Phase
Science Instrument	Imaging Camera (5)	0	+20	Science
Power	EPS + Battery	-40	+85	All
TT&C	Transceiver + OBC (rx: 10, rx+tx: 25)	-30	+70	All
Propulsion	Thruster	~ 0	~ +90	Burn
Data Processing	Processor	-40	+60	All
ADCS	Reaction Wheels (8)	-40	+70	All
ADCS	Microthrusters	0	+60	All
ADCS	Star Tracker	-20	+50	All

The active thermal management system will feature one thermistor per subsystem to measure temperature and autonomously control the operation and scheduling of subsystems. To keep the hyperspectral imager within its operating temperature range during the science phase, high-power systems such as the transceiver will be restricted to receive mode. When the spacecraft is in a low power mode or in eclipse a battery heater will maintain the minimum temperatures.

4.8. Assembly, Integration, & Testing

The assembly, integration, and test phase of the Mini-Luna mission's TReX spacecraft involves thorough planning and execution to ensure the spacecraft meets stringent mission requirements. Key considerations include the selection of appropriate materials and the precise placement of components to optimize performance and reliability. For the frame structure, Aluminum 6061-T6 was chosen for its mechanical properties, machinability, and manufacturability, crucial for achieving payload efficiency and launch compatibility. Component placement is strategically planned to enhance operational efficiency and minimize risks during launch and mission phases. The center of mass (COM) is strategically positioned near the edge that connects to the launch vehicle, mitigating potential buckling loads and undesirable rotations. Deployable solar panels are located on the sides to maximize power generation, while antennas are placed on the upper and bottom side for optimal communication capabilities. Meanwhile, the thruster is situated near the surface that is aligning with its attachment point to the launch vehicle, ensuring stability and controlled maneuverability during flight. A four-view and exploded view of the TReX concept is depicted in Figures 8 and 9.

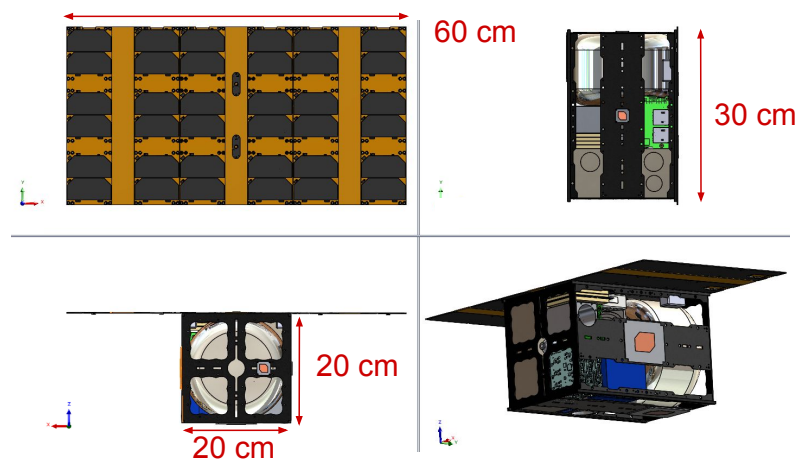


Figure 8: TReX Four-View.

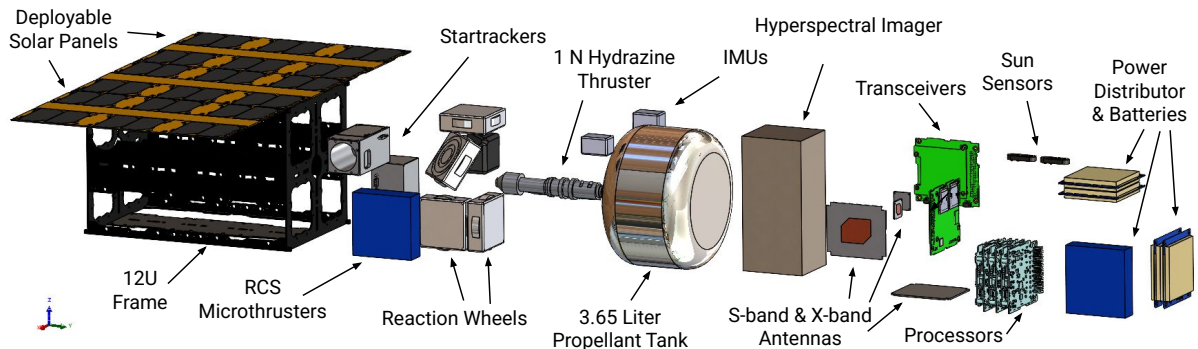


Figure 9: TReX Labeled Subsystems & Components.

The testing plans in Figure 10 for the TReX spacecraft encompasses comprehensive subsystem and system-level evaluations to validate functionality, endurance, and readiness for space deployment. Subsystem testing begins with unit tests to assess individual component performance, followed by module tests to verify integrated subsystem functionality. Stand-alone functional tests then ensure each subsystem operates independently and cohesively within the spacecraft architecture. Additionally, a critical step in the subsystem testing phase involves bakeout procedures, where components undergo heating within a vacuum chamber to eliminate volatiles and prevent outgassing that could affect mission operations in space.

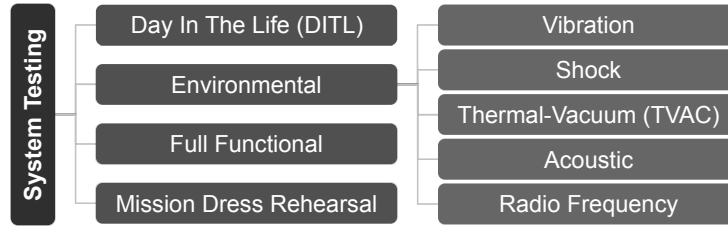


Figure 10: Future Test Plans.

System integration marks the next phase, where all subsystems are integrated into the spacecraft platform to ensure seamless interaction and compatibility. This integration phase sets the stage for rigorous system-level testing, including the Day In The Life (DITL) test to simulate operational scenarios and deployment sequences. Environmental tests are then conducted to expose the TReX spacecraft to simulated launch and space conditions, such as vibration testing on shaker tables and thermal-vacuum tests (TVAC) to simulate extreme temperature variations. Acoustic tests further evaluate the spacecraft’s ability to withstand launch acoustic environments, while Radio Frequency (RF) tests ensure optimal performance of communication and antenna systems. In addition, A Hardware-In-The-Loop simulation should be developed to accurately replicate key mission scenarios, preventing issues like reaction wheel assembly saturation by simulating IMU outputs. A full functional test culminates the testing phase, exercising all operational modes and functions to confirm the spacecraft’s readiness for its mission objectives. Finally, a mission dress rehearsal test involves a complete run-through of mission operations and ground station interactions to verify mission readiness before launch.

This systematic approach to assembly, integration, and testing ensures that the Mini-Luna TReX spacecraft is robust, reliable, and fully prepared to undertake its pioneering mission to study TCO, contributing valuable insights into solar system formation and evolution.

5. Cost Estimation and Risk Analysis

Table 11: Total Cost Breakdown.

	Labor	Instrument	Reserve [%]	Total (FY2024)
Ground System & Comms	\$229,433	\$50,000	30	\$363,262
Data Processing	\$229,433	\$6,000	15	\$270,747
Attitude Dynamics & Control	\$229,433	\$395,000	15	\$718,097
Instrumentation	\$229,433	\$1,000,000	15	\$1,413,847
Propulsion and Launch	\$229,433	\$250,234	30	\$623,566
Environmental Protection	\$229,433	\$2,500	15	\$266,722
Power	\$229,433	\$150,000	30	\$493,262
Integration and Testing	\$305,910	\$513,800	30	\$1,065,623
Systems Engineering	\$229,433	\$0	15	\$263,847
TOTAL Satellite Cost:		\$2,367,534		
Management & Mission Assurance	\$1,300,118		30	\$1,690,153
RideShare	\$0		0	\$0
Facilities	\$1,000,000		15	\$1,150,000
Operations	\$815,760		15	\$938,124
Network Usage	\$407,880		30	\$530,244
TOTAL	\$8,032,661			\$9,787,496

The mission must not cost more than \$55 million. To adhere to this requirement, preliminary calculations were conducted by first analyzing the cost per subsystem for a single satellite, as well as the associated costs for management, systems engineering, and operations. A reserve was added to each subsystem based on its cost risk: 15% for low-risk, 30% for medium-risk, and 50% for high-risk subsystems. Expenses related to wages, human resources, and operational activities were also accounted for in addition to these subsystem costs. Wages were estimated based on contemporary start-up company

aerospace engineer salaries. The final estimated cost for the mission was approximately \$9.787 million. Table 11 shows a detailed breakdown of the total cost. Table 12 shows the cost, mass, and volume with respect to the constraints of NASA's SIMPLEX program.

Table 12: Constraint and Total Budget Breakdown.

	Constraint	Total
Cost	\$55 M	\$9.787 M ± 0/1.755 M
Mass	24 kg	15.34 ± 0/1.61 kg
Volume	12,000 cm ³	11,705.4 ± 0/906.7 cm ³

5.1. Size, Weight and Power (SWaP)

TREx is a CubeSat mission developed in compliance with the NASA SIMPLEX solicitation requirements. As such, it is subject to strict size and mass constraints, more specifically, a total mass under 24 kg and a volume not exceeding 12U [6]. Managing SWaP constraints in a CubeSat designed to rendezvous with an asteroid, capture images, and transmit them back to Earth from a distance of approximately 2 million kilometers presents significant engineering challenges.

Table 13: Size and Weight per Component.

Subsystem	Component	Mass				Volume			
		Est. (g)	Est. (kg)	Margin [%]	Total (kg)	Est. (cm ³)	Est. (U)	Margin [%]	Total (U)
Ground System & Comms	X-Band Antenna (x2)	6.0				30.0			
	S-Band Antenna (x2)	128	0.73	25	0.91	30.0	0.3703	5	0.3888
	Transceiver (x2)	600				310.3			
Data Processing	Processor (x3)	192	0.19	25	0.24	465.4	0.465	5	0.489
Attitude Dynamics & Control	Rxn Wheels (x4)	1320				490.0			
	Microthrusters	542				237.1			
	Star Tracker (x2)	700	2.69	5	2.83	550.0	1.28	5	1.34
	Sun Sensor (x2)	20				0.007			
	IMU (x2)	110				0.07			
Payload	Hyperspec. Imager	1250	1.25	5	1.31	1350	1.35	5	1.42
Propulsion	Propellant	3081				3081			
	Propellant Tank	1100				569			
	Piping & Fittings	400	4.83	15	5.56	500	5.50	10	6.05
	Thruster	250				1350			
Environmental Protection	Frame	2440				323			
	Coatings	100	2.54	15	2.92	4.98	0.33	10	0.36
Power	Solar Panels (x3)	823				324.8			
	Distributor	100				535.7			
	Batteries	430	1.50	5	1.58	397.4	1.51	10	1.66
	Wiring Harnesses	150				250.0			
TOTAL:			13.74		15.34		10.80		11.71

For this mission, volume ended up being the biggest limiting factor. TREx will rely entirely on a chemical propulsion system to meet its high delta-v requirement of 529 m/s, which alone demands approximately 6U of volume. The power, ADCS and payload subsystems each required between 1-1.5U. A detailed breakdown of each subsystem's volume and mass allocation is provided. A detailed power budget per mission phase is found in the previous section for the power subsystem.

Table 13 shows that the estimated mass of TREx is 13.78 kg. When accounting for margins, this increases to 15.34 kg, which remains comfortably within the 24 kg maximum imposed by the SIMPLEX solicitation. The estimated volume is 10.80U though accounting for margins raises it to 11.71U. With a maximum volume constraint of 12U, design decisions must continue to trend towards less volume additions in order to maintain requirements compliance.

5.2. Risk

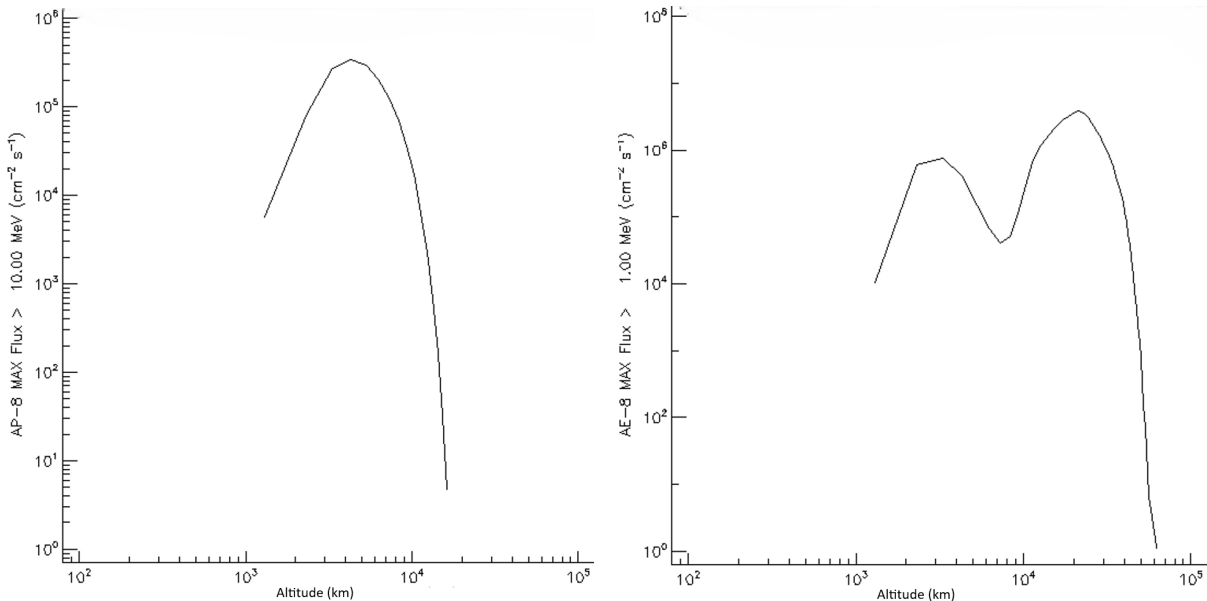
The mission includes numerous sources of risk, some more consequential than others. Table 14 has these risks, while Table 15 is the Risk Matrix, or a diagram that shows significant risks at various levels of consequence and likelihood for the mission.

Table 14: Risks to Mini-Luna Mission.

ID	Mitigation	Description
A	LSST	No suitable TCO for rendezvous (Traj.)
B	COTS	Mission cost over budget (PM)
C	Testing	Antenna deployment failure (Comms)
D	Testing/TRL	Solar panel deployment failure (Power)
E	Cycle Burn	Thruster overheating (Thermal)
F	Redundancy	Reaction wheel failure (ADCS)
G	TRL 9	Thruster system failure (Prop)
H	Testing/Rad Hard	Component radiation damage (FDIR)
I	Outsource	Mission timeline slip (PM)

Table 15: Risk Matrix.

		Consequence			
		Low	Med	High	High
Likelihood	High	B	E	I	
	Med	F	A	G	C, D
	Low			H	
	Low				



(a) Proton flux (AP-8) for energies > 10 MeV (b) Electron flux (AE-8) for energies > 1.0 MeV

Figure 11: Radiation belt flux models showing energetic proton and electron populations in geocentric orbit.

One risk that was considered is instrument failure due to highly charged radiation particles from the space environment. Radiation shielding was evaluated for TReX. The Van Allen belts, regions of energetic electrons trapped by Earth’s magnetosphere and originating from solar wind, pose a significant hazard to spacecraft. Electronic components can experience Single Event Upsets (SEUs), such as memory bit flips or gate ruptures, as well as gradual performance degradation from sustained exposure. These belts extend from roughly 640 km to 58,000 km above Earth’s surface. However, since TReX will be deployed via a rideshare to the Earth-Moon L2 point, approximately 1.5 million kilometers away, the belts will have no direct impact on the mission, as shown in Figure 11 where it can be appreciated that TReX avoids these zone. Any necessary shielding during transit will be the responsibility of the rideshare vehicle.

While radiation is not expected to pose a significant threat to TREx, the ESP-PSYCHIC tool from the Space Environment Information System (SPENVIS) [21] was still used to estimate solar proton fluence and assess potential exposure. The total radiation dosage for an Aluminum sphere was taken as representative of spacecraft radiation dosage to constrain the shielding requirements. A shielding of about 2 mm reduces the dosage by two orders of magnitude below 10 krad. Generally, COTS components are radiation hardened, and the OBC can withstand total ionization dosage (TID) values up to 10 - 15 krad [22]. Table 16 collates aspects of each component in regards to radiation tolerance.

Table 16: Component Radiation Tolerant Qualifications.

	Total Dose	Comments
Processor	30 krad	Total ionizing dose (TID)
Flash FPGA	20-30 krad	Worst-Case SEU of $1 \cdot 10^{-10}$ errors/bit-day
Sun Sensor	30 krad	Proton beam energy of 6 MeV
EPS Power Module	20 krad	-

5.3. Fault Detection, Isolation, & Recovery (FDIR)

FDIR is a contemporary methodology to prevent a spacecraft loss of mission (LOM). System autonomy plays a major part in space mission FDIR operations, thus bringing about fault management and system autonomy (FMSA). It is imperative to monitor for potential failure modes such as radiation-related faults or anomalies related to power, thermal regulation, attitude control, communication, and software integrity. Once detected, the system should isolate where the fault occurred and get the spacecraft back to a deterministic safe state. There are a variety of ways to design and analyze a spacecraft's FDIR ability. A spacecraft can be designed from the beginning of the design review process to prevent emergent failure modes. An architecture may include redundant subsystems, components, or harnesses. If the architecture is unable to be physically changed, then flight software (FSW) can provide the necessary actions needed to recover nominal functionality.

Table 17: Component-Level Redundancy.

	Value	Min.	Redundancy	Fault Tolerance
Processors	3	1	$n + 2$	Dual
Flash FPGA Pathways	2	1	$n + 1$	Single
Reaction Wheel Triad	4	3	$n + 1$	Single
Star Tracker	2	1	$n + 1$	Single
Sun Sensor	2	1	$n + 1$	Single
IMU	2	1	$n + 1$	Single
EPS Kill Switches	2	1	$n + 1$	Single
Solar Panels	3	2	$n + 1$	Single
Thruster	1	1	n	Zero
Thruster Heaters	2	1	$n + 1$	Single
X-Band Transmitter	2	1	$n + 1$	Single
S-Band Transmitter	2	1	$n + 1$	Single
Transceiver	2	1	$n + 1$	Single
Science Instrument	1	1	n	Zero

Cubesats do not usually have the cost or schedule incentives to implement rigorous FDIR features. One of the main benefits of a cubesat architecture is the low financial risks. The Mini-Luna mission is unique in that the spacecraft is of the cubesat form factor while benefiting from a higher financial budget. Due to the SIMPLEx solicitation's ample budget, the team can increase redundancy and FDIR options. The spacecraft is constrained to the 12U size which is an active constraint of the design; this leads to the interest in FDIR methods that do not take up more volume than needed. FSW FDIR can improve the chances of mission success for Mini-Luna. Another potential option is utilizing redundancy of small components; Table 17 shows this component redundancy.

Each subsystem has a variety of FDIR aspects taken into account. The spacecraft will have three processors, where two run simultaneously in a Hot-Hot-Standby configuration. On-board processes are separately completed twice in this configuration. The two outputs will be compared between each

other and one of the outputs will be discarded in the event of a mismatch with the other two. After some persistence of an out-of-bounds output, one of the processors will be reset. Processing will be in a Hot-Standby-Standby configuration until mission operators give the faulted processor the go-ahead to reintegrate into the system. Each individual processor includes redundancy, EDAC-protected RAM, upset and multi-current monitoring, multiple overcurrent protections, FPGA bit-stream scrubbing, and built-in watchdogs/software monitoring. The two star trackers can be operated in parallel to increase the positional accuracy of the spacecraft. The EPS power module has memory code integrity verification using a checksum, as well as a programmable watchdog timer. The communication subsystem has two of each antenna and transceiver, where the secondary components are backups.

6. Conclusion

This paper explains a mission concept for cislunar asteroid imaging, emphasizing a small form factor to accomplish mission objectives. The Mini-Luna mission with its TCO Rendezvous Explorer (TREx) fits within the constraints of NASA's Small Innovative Mission for Planetary Exploration (SIMPLEx) program while aiming to address fundamental questions outlined in the National Academy of Sciences, Engineering and Medicine 2023-2032 Decadal Survey. Scientific instrumentation and intended data collection will help answer key questions about the evolution of the solar system and the universe.

Science goals include understanding of the nebula's solid and gas radial mixing, planetesimal formation, small body dynamical evolution, and life cycles of small bodies. These goals connect to the science objective of characterizing the internal structure, determining the size, shape, and rotation rate, and characterizing the surface composition of minerals and volatile compounds of a temporarily-captured orbiter (TCO). This will be achieved through the use of visible and IR spectrometer. While a small form factor like a CubeSat challenges mission feasibility, the SIMPLEx program provides support favorable for the Mini-Luna mission.

Acknowledgments

The authors would like to express our deepest appreciation to our mentors, Professors James Lloyd, Dmitry Savransky, Elaine Petro, Greg Falco, Fabien Royer, and Andrew van Paridon. The authors would additionally like to thank the Cornell Smallsat Mission Design School (SMDS) teaching assistants Grace Genszler and Joshua Umansky-Castro. This SMDS program research was funded by: Boeing, Millennium Space Systems: A Boeing Company, AVS US, Voyager Space, Moog Space and Defense Group, NASA New York Space Grant Consortium, Cornell's College of Arts & Sciences, and Cornell Engineering Sibley School of Mechanical & Aerospace Engineering.

References

- [1] National Academies of Sciences, Engineering, and Medicine and others, *Origins, worlds, and life: a decadal strategy for planetary science and astrobiology 2023-2032* (2022).
- [2] P. Brown, R. Spalding, D. O. ReVelle, E. Tagliaferri, S. Worden, The flux of small near-earth objects colliding with the earth, *Nature* 420 (2002) 294–296.
- [3] National Aeronautics and Space Administration (NASA), *NASA Planetary Defense Strategy and Action Plan, 2023*. In support of the National Preparedness Strategy and Action Plan for Near-Earth Object Hazards and Planetary Defense.
- [4] A. Lue, J. D. Ruprecht, J. Varey, M. Czerwinski, H. E. M. Vighh, Discovering the smallest observed near-earth objects with the space surveillance telescope, *Icarus* 325 (2019) 105–114.
- [5] R. L. Jones, M. Jurić, Ž. Ivezić, Asteroid discovery and characterization with the large synoptic survey telescope, *Proceedings of the International Astronomical Union* 10 (2015) 282–292.
- [6] NASA Headquarters, *NASA Small Innovative Missions for Planetary Exploration (SIMPLEx)*, European Planetary Science Congress, Vol. 12, No. EPSC2018-1074 (2018).
- [7] Greshko, M., *NASA's Moon Program Faces Delays. Its Ambition Remains Unchanged*, (2024) Retrieved 16 July 2024 <https://www.scientificamerican.com/article/nasas-moon-program-faces-delays-its-ambition-remains-unchanged/#:~:text=Artemis%20III%E2%80%94the%20program's%20first,the%20program's%20history%20and%20ambition>.
- [8] NASA, U.S. Government, *Orbital Debris Mitigation Standard Practices*, November 2019 Update, 2019. Accessed 14 March 2025.
- [9] G. H. Jones, C. Snodgrass, C. Tubiana, M. Küppers, H. Kawakita, L. M. Lara, J. Agarwal, N. André, N. Attree, U. Auster, et al., The comet interceptor mission, *Space science reviews* 220 (2024) 9.
- [10] S. Brelsford, M. Chyba, T. Haberkorn, G. Patterson, Rendezvous missions to temporarily captured near earth asteroids, *Planetary and Space Science*, 123 (2016) 4–15.
- [11] National Aeronautics and Space Administration, *NASA to Track Asteroid 2024 PT5 on Next Close Pass, January 2025*, (2024) Retrieved 3 March 2025 <https://blogs.nasa.gov/planetarydefense/2024/10/02/nasa-to-track-asteroid-2024-pt5-on-next-close-pass-january-2025/#:~:text=Estimated%20to%20be%20about%2033,from%20Earth%20than%20the%20Moon>.

[12] National Aeronautics and Space Administration, 2024 YR4 ((2025) Retrieved 3 March 2025 <https://science.nasa.gov/solar-system/asteroids/2024-yr4/>).

[13] Jet Propulsion Laboratory, Horizons System, (2025) Retrieved 3 March 2025 <https://ssd.jpl.nasa.gov/horizons/>.

[14] D. C. Folta, T. A. Pavlak, A. F. Haapala, K. C. Howell, M. A. Woodard, Earth-moon libration point orbit stationkeeping: Theory, modeling, and operations, *Acta Astronautica* 81 (2013) 323–335.

[15] M. Cardì, M. Pavoni, D. Calvi, A. Zanotti, F. Corradino, E. Sanguineti, F. Nichele, F. Topputo, F. Ferrari, C. Giordano, et al., The hera milani mission, in: *Small Satellites Systems and Services Symposium (4S 2024)*, volume 13546, SPIE, pp. 677–691. (2025).

[16] D. Korda, A. Penttilä, A. Klami, T. Kohout, Neural network for determining an asteroid mineral composition from reflectance spectra, *Astronomy & Astrophysics* 669 (2023) A101.

[17] T. Kohout, D. Korda, A. Penttilä, L. Rajamäki, L. Palamakumbure, Detection of composition, space weathering, and local resurfacing using aspect hyperspectral imager of esa hera/milani mission, in: *European Planetary Science Congress*, pp. EPSC2024–316. (2024).

[18] C. R. Chapman, J. W. Salisbury, Comparisons of meteorite and asteroid spectral reflectivities, *Icarus* 19 (1973) 507–522.

[19] A. Cervone, F. Topputo, S. Speretta, A. Menicucci, E. Turna, P. Di Lizia, M. Massari, V. Franzese, C. Giordano, G. Merisio, D. Labate, G. Pilato, E. Costa, E. Bertels, A. Thorvaldsen, A. Kukhareuka, J. Vennekens, R. Walker, Lumio: A cubesat for observing and characterizing micro-meteoroid impacts on the lunar far side, *Acta Astronautica* 195 (2022) 309–317.

[20] NASA Deep Space Network (DSN), Deep Space Network (DSN) Radio Astronomy User Guide, (2021). Retrieved 14 March 2025.

[21] D. Heynderickx, B. Quaghebeur, E. Speelman, E. Daly, Esa’s space environment information system (spenvis): a www interface to models of the space environment and its effects, (2000).

[22] W. Treberspurg, A. Rezaei, R. Kralofsky, A. Sinn, A. Stren, C. Scharlemann, Radiation tests of a cubesat obc, *Advances in Space Research* 74 (2024) 1253–1260.

Appendix

Table 18: Science Traceability Matrix (STM).

Science Goals	Science Objectives	Scientific Measurement Requirements		Instrument Performance Requirements		Est. Instrument Performance	Mission-Level Requirements
		Physical Parameters	Observables	Description	Requirement		
Q4.1b How Has Collisional and Dynamical Evolution Affected Small Body Populations	Determine the size, shape and rotation rate of the TCO	1. Diameter and shape of TCO 2. Rotational speed and time period of rotation					
Q4.1c What Are the Life Cycles (Physical States and Rotational Properties) of Small Bodies in the Solar System and How Are They Affected by Collisions, Thermal Changes, and Non Gravitational Forces?	Characterize the surface composition of minerals, and volatile compounds	1. Surface elemental composition and inventory of volatile 2. Surface roughness 3. Surface temperature map and thermal anomalies	1. Time series of lightcurve 2. Multispectral images of reflectance spectra in Vis-NIR, SWIR Fe2+ absorptions in 1-2 μm Fe3+ absorption in hydrated silicates at ~0.7 μm OH-absorption at ~1.4 μm H2O absorption at ~1.9 μm	Multispectral imager and spectrometer operating in Vis-NIR wavelength range e.g. Hera Milant ASPECT	1. Spectral range: 700 nm to 1700 nm 2. Image resolution: Less than 0.01 m/px 3. Vis bandwidth less than 40 nm [Mastcam Z] 4. NIR bandwidth less than 50 nm [Hayabusa AMICA] 5. SNR: 30 [Mastcam Z]	ASPECT Flight heritage: Hera mission VIS: 500 – 900 nm, res: less than 20 nm NIR1: 850 – 1275 nm, res: less than 40 nm NIR2: 1225 - 1650 nm, res: less than 40 nm SWIR: 1600 - 2500 nm, res: less than 40 nm SNR: 30-70 [Achieved after denoising] Mass: 1.25 kg Power: 13-14 W Size: 12.8 x 9.6 x 10 cm ³	TREx shall target a TCO at least 1 meter in diameter as estimated by ground observation. TREx shall match the trajectory of the target TCO at a distance of no more than 50 m. TREx shall control its position and attitude while imaging the target TCO such that its science payload is facing the TCO's illuminated face. TREx shall conduct the science phase of its mission for at least 10 hrs timespan. TREx shall communicate payload data to the ground segment subsequent to science data capture and processing. TREx shall enter an appropriate EoL trajectory subsequent to confirmation of payload data receipt from the ground segment.